16th Australasian Fluid Mechanics Conference
Crown Plaza, Gold Coast, Australia
2-7 December 2007

On the Effects of Droplet Loading on the Structure of Spray Jets

J.D. Gounder, A.R. Masri and S. Starner

School of Aerospace, Mechanical and Mechatronic Engineering,
University of Sydney, New South Wales, 2006 AUSTRALIA

Abstract

This paper uses advanced laser diagnostics to investigate the effects of droplet loading on the structure and mixing patterns of sprays in a non-reacting, turbulent jet. A nozzle designed at University of Sydney with the objective of studying spray flames has been used for producing a two phase flow in a co-flowing air stream with well defined boundary conditions. Varying the quantity of liquid injective will vary the number density of the droplets in the flow.

The co-flowing air stream is seeded with a fixed concentration of nitric oxide, NO which will act as a conserved scalar. Laser induced fluorescence of NO is exploited to provide a direct quantitative measure of the mixture fraction. Radial profiles of the mean and the rms of mixture fraction has been collected at various axial positions in jets with different spray loadings. It is found that mixture fraction profiles are different from those measured in turbulent gaseous jets and increasing the droplet loading increases the mixture fraction of the jet due to evaporating droplets.

Introduction

Spray flows are common in many industrial applications ranging from chemical processing to burners, gas turbine combustors and internal combustion engines. The physics and chemistry of spray flows in these applications are made complex by the unknown interactions between the droplets, the turbulence, mixing and chemical processes. Accurate models are needed to study these phenomena's and improve future designs of these spray systems. Due to scarcity of detailed experimental data that isolate each of the complex features of a spray, which include droplet size, velocity, evaporation, droplet interaction with gas flow, turbulence, mixing and chemical reaction, has made it difficult to validate such models. Faeth, [1, 2] has reviewed previous work on spray combustion and has listed a number of databases for flows involving sprays.

The spray combustion project at the University of Sydney is dedicated to developing an improved understanding of spray jets and flames and to developing a comprehensive database in a laboratory burner that is experimentally tractable as well as numerically simple enough to isolate effects of turbulence, evaporation, mixing, droplet interactions, and chemical reactions. Previous papers by Chen *et al*, [3-6] provide initial data for sparsely loaded spray jets, where fine sprays created by air blast generated droplets in a glass nebuliser. The Sauter mean diameter ranges from 14 to 35 microns. Starner *et. al*, [7] then measured droplet size and velocity in a sparsely loaded piloted spray flame, where the droplets in the spray was created using a ultrasonic nebuliser, which is more akin to sprays seen in industrial applications.

This paper is the continuation of the on going work to study the mixing behaviour of a spray loaded turbulent jet. As reported previously a technique has been developed [8] to measure vapour phase mixture fraction in a spray jet. Nitric oxide, NO is seeded in the coflow shrouding the jet. Mass fraction of NO is used as a conserved scalar, Zi in determining the mixture fraction, ξ

$$\xi_{coflow} = \frac{Z_i - Z_{i,2}}{Z_{i,1} - Z_{i,2}} \tag{1}$$

where subscripts 1 and 2 denote the fuel and oxidiser streams [9]. The mixture fraction of the jet stream is then given by 1-ξ_{colfow}.

Laser induced fluorescence of NO has been used extensively in many single-point and imaging applications. Barlow *et al* [10, 11] have measured nascent NO at single points in turbulent flames while Laurendeau's group has seeded NO in premixed flames of varying stoichiometries and studied its interaction with the flows. The objective of these studies and others [12-17] was to develop the LIF-NO technique as temperature diagnostic tools using the ratio of one or more NO fluorescence lines. For the present study, LIF signal from NO is used for determining the mass fraction of NO and thus the mixture fraction in a turbulent jet loaded with spray droplets. The excitation line used is the Q_1+P_{21}(14.5) transition of the A-X(0,0) band at 226.03 nm.

Mixing fields in axisymmetric gaseous jets have been studied by many researchers. Antonia *et al*, [18] has studied heated round gaseous jets, provided the mixing fields using temperature as the conserved scalar. Pitts [19, 20] and Mi *et al* [21] have carried out extensive work on axisymmetric jets, the former studying the effects of global density ratio and Reynolds number on the centreline mixing behaviour and the later studying mixing characteristics of jets from contoured nozzle, an orifice and a pipe. Measurements in sprays jets are compared to those obtained earlier for gaseous jets to highlight the effects of sprays on the mixing structure.

Experimental Setup

The schematic diagram of the experimental setup is given in [8]. Excitation wavelength for NO LIF is generated by employing the second harmonic (λ = 532nm) of a Quanta-Ray Pro-Series Pulsed Nd:YAG laser to pump a Sirah dye Laser , which provides visible radiation at 622.18nm. The dye laser fundamental is sum frequency mixed with the frequency tripled Nd:YAG laser beam (355nm) to obtain UV light at 226.03nm. The excited beam was spatially separated from the residual beams using Pellin-Broca prisms. The laser energy was 9.3mJ/pulse. The laser beam was focussed into a sheet of thickness 200 microns using a 400 mm focal length cylindrical lens.

The fluorescence signal corresponding to the γ(0,1) band of NO was collected on an intensified flow master CCD camera. The signal was filtered using a short wave pass dichroic filter transmitting light at 236nm with a bandwidth of 10nm. A custom made filter made by BARR Associates was used for filtering strong Mie signal from the droplets. This long pass filter had a optical density of over 5 at 226nm and 59% transmittance at 236 nm. The object size of the raw images is 32x25 mm. The images are taken at a range of axial positions ranging from x/D = 0 to x/D=20. A second Flow Master camera is used for monitoring the laser energy on a shot to shot basis.

Spray Burner

A 3D schematic of the burner setup is shown in figure 1a. The burner nozzle and coflow assembly is mounted inside a 29 x 29 cm vertical wind tunnel. The outlet of the wind tunnel has screens mounted on it to smooth out the flow. The inside diameter of the coflow is 104 mm. In unconfined flows, air would be entrained from the surrounding into the co-flowing stream hence reducing the region where the initial boundary conditions prevail. Moreover, the entrained air is not seeded with NO hence un-validating its use as a conserved scalar. To prevent this, shrouds are added to isolate the seeded co-flow from the surrounding up to the measurement location. These co-flow shroud extensions are used for x/D equals 5, 10, 15 and 20, where x is the axial distance from the jet exit plane. The lengths of these extensions from the jet and coflow exit planes are 32.5, 72.5, 123.5 and 174.5 mm for the respective x/D positions. At x/D = 0 the jet and the coflow have the same exit plane as shown in figure 1b. Meshed wire screens are used in the coflow to smooth out the flow and give a top hat velocity profile at the exit plane. The diameter of the jet is 10.5 mm.

(a)

(b)

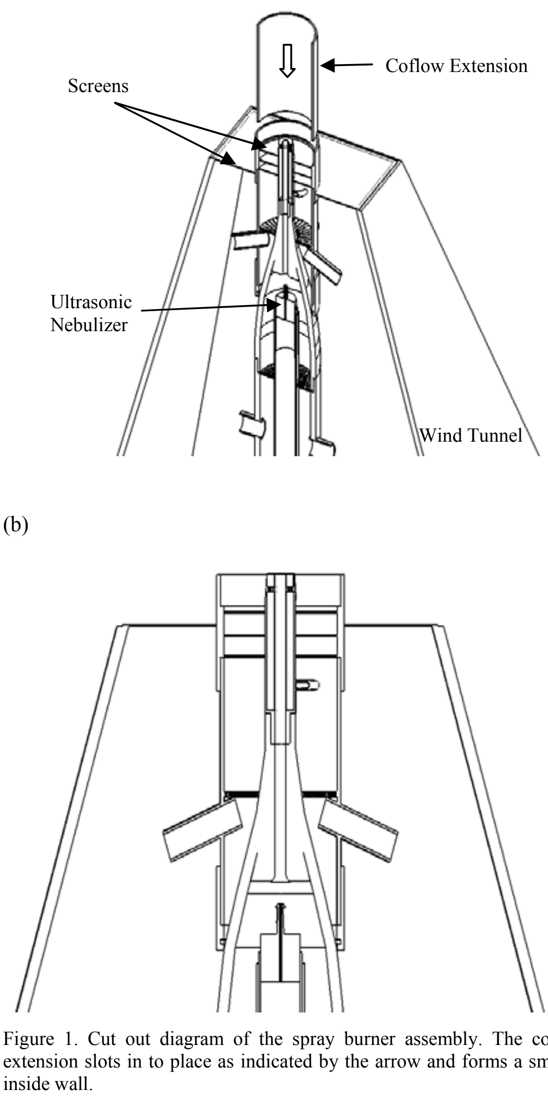

Figure 1. Cut out diagram of the spray burner assembly. The coflow extension slots in to place as indicated by the arrow and forms a smooth inside wall.

Initial Conditions

The bulk velocity of the coflow, pilot and the wind tunnel is 3 m/s. Nitric oxide, NO is seeded at 200ppm in the coflow and pilot streams. Table 1 gives a summary of the four cases studied here. The first case is an air jet, where L stands for low jet carrier velocity and A for Air without spray. Cases LL LM and LH are the 3 air jets with spray, where the second letters L, M and H denotes droplet loading of low, medium and high. Ultrasonically generated droplets with near zero momentum are entrained in the carrier stream. The droplet loading is varied by varying the mass flow rate of the liquid acetone. Flow rates were measured using rotameters, tri-flats and Tylan electronic mass flow meters.

Case	Air volume flowrate l/min	Acetone mass flowrate kg/min
LA	114.3	0
LL	114.3	0.024
LM	114.3	0.045
LH	114.3	0.075

Table 1. Air and fuel flow rates for 1 air and 3 spray jet cases.

Air Jet Flow Simulation

The commercially available computational fluid dynamics package Fluent is used to perform computations of simple gaseous jets that are used as a baseline for comparison with measurements. Fluent is widely used and has therefore undergone extensive testing making it particularly useful for this type of simulations. The computation domain size is 500 mm x 145 mm. The colfow wall had a extension of length 275 mm similar to the experiment. A staggered grid with 73000 cells is used for the computation. All calculations are solved assuming steady flow. The model used is axisymmetric standard k–ε. Dally *et al*, [22] has shown that the k–ε model over predicts the decay rate and the spreading rate for a round jet. Dally concluded that using $C_{\varepsilon 1}$ = 1.6 gave a better representation of the decay and spreading rate for a round jet. Therefore constants $C_{\varepsilon 1}$ and $C_{\varepsilon 2}$ used are 1.6 and 2.02.

Argon has been used as a marker of mixture fraction in the calculation of an air jet issuing in air co-flow. Argon, at 200ppm is seeded in the colfow and pilot to simulate Case LA. A no slip boundary condition has been used for the walls of the jet, pilot, coflow, and the wind tunnel. The boundary conditions are given in table 2. The solution converged after 2300 iterations.

Jet Inlet Mass flow rate kg/s	0.0024799
Turbulent intensity %	14
Pilot Inlet Velocity m/s	3
Turbulent intensity %	3
Coflow Inlet Velocity m/s	3
Turbulent intensity %	3
Wind Tunnel Inlet Velocity m/s	3
Turbulent intensity %	3

Table 2. Boundary condition for Case LA for Fluent simulation.

Results

Validation with Air Jet

The validity of the NO LIF technique is confirmed first by comparing the measurements made in gaseous jets with other experiments made in similar flows as well as with calculations. Case LA is used here as a baseline and Fig. 2 shows the centreline axial decay of mean mixture fraction for the current measurements compared with two other data sets reported in the literature. Antonia, [18] and Mi, [21] have shown an x^{-1} dependence of mean centreline mixture fraction. The current experiment data shows a similar dependence. The axial decay of mixture fraction for Case LA from the Fluent simulation also follows a similar trend. The simulations also show a 1/x dependence of mean mixture fraction.

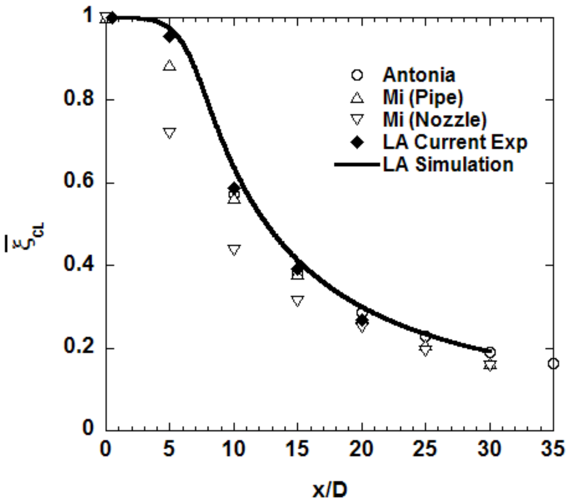

Figure 2. Mean centreline decay of mixture fraction in a axisymmetric air jet. Both experiment and simulation show similar trends that $\xi_{CL}(x) \sim (1/x)$.

Comparison of the radial profiles of the mean mixture fraction at x/D = 0.5, 5 10, 15 and 20 between current experiment and the simulations is shown in figure 3. The simulation is predicting slightly faster spreading rate compared to the experiment for x/D 5 and 10. This could be due to the value of the constants for generation $C_{\varepsilon1}$, and destruction $C_{\varepsilon2}$, of the turbulent dissipation term used for these calculations. For x/D = 15 and 20 the radial profiles from the experiment and the simulation look much closer.

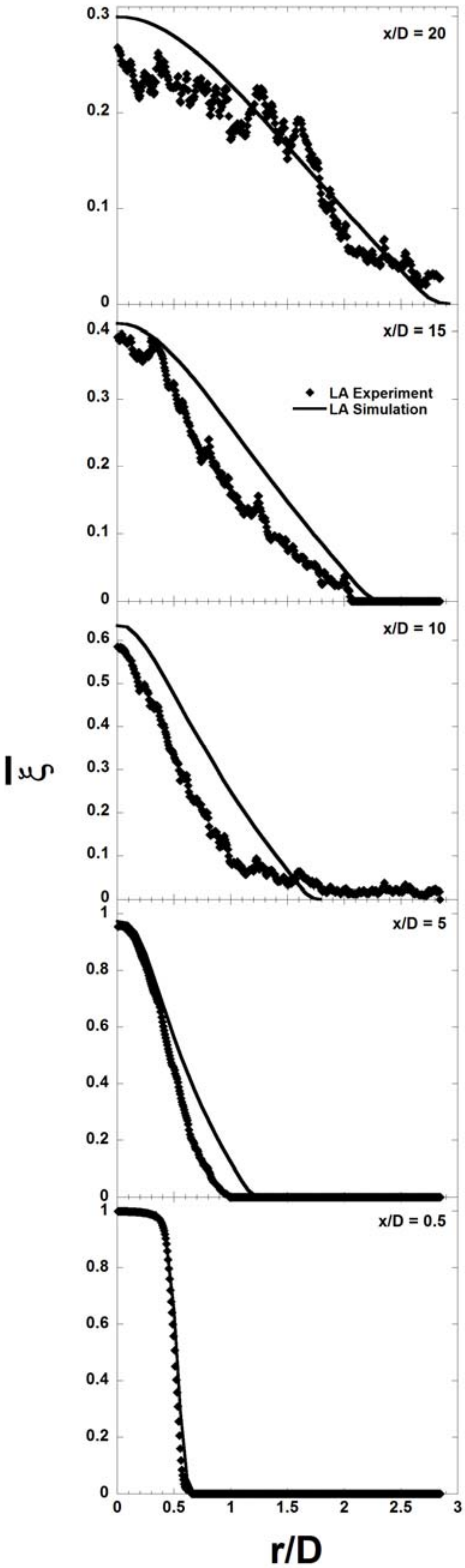

Figure 3. Comparison between radial distributions of mean mixture fraction for the air jet case LA, measured using the NO LIF technique and calculated via Fluent simulations.

Mixture Fraction Fields in Spray Jets

Figure 5 and 6 show 2D instantaneous field of mixture fraction for cases LA LL LM and LH at five axial stations. The individual image size is 32 mm x 10 mm. At the jet exit plane the mixture fraction is unity as shown by the images. There are small rolling eddies forming at the edge of the jet which entrains air from the pilot and coflow streams. The bulk jet velocity is constant and hence the structure of the rolling eddies at x/D = 0 for all the cases are similar. Few droplets are visible for cases LL LM and LH at the exit plane too.

As the jet spreads larger eddies are visible further downstream. These eddies increase the entrainment of coflowing air, which then reduces mixture fraction in the air jet, LA but increases the evaporation of the spray droplets in the spray jets LL, LM and LH and thus giving higher mixture fraction. The high mixture fraction is due to the increase in vapour concentration which slows down the diffusion of coflow air into the core of the jet. There are air pockets that get entrained in the jet and some move to the centre of the jet. Droplets can be seen at downstream locations. The images also show that the spray loaded jets have a larger spread rate compared to the air jet. This could be due to the existence of droplets.

The higher spreading rate of the spray loaded jets can be confirmed by the radial profiles of mean mixture fraction plotted in figure 7. At x/D = 0.5 and 5 there is no difference in the radial profiles of mean mixture fraction for the 4 cases except the centreline values. A small increase is observed in mixture fraction for cases LL, LM and LH at x/D = 10, with case LL showing the largest change. This could be due to low droplet number density and thus higher evaporation rate. At x/D = 15 and 20 the mixture fraction of the LH and LM cases increase with LH being the higher one. The radial profiles show that the air case LA has the lowest mixture fraction and it increases with the droplet loading.

The mean centreline decay of mixture fraction, $\bar{\xi}_{CL}$ for the spray cases LL, LM and LH are compared with the air case LA in figure 4. The profiles of $\bar{\xi}_{CL}$ for cases LL LM and LH increase as x/D increases. For x/D = 0.5 and 5, $\bar{\xi}_{CL}$ for case LA is higher. At x/D = 10 all 4 case have almost similar $\bar{\xi}_{CL}$ values. A distinct difference in $\bar{\xi}_{CL}$ can be seen at x/d = 15 and 20. The LH case has a higher mixture fraction value at x/d= 15 compared to LL, LM and LA and as the x/D increases to 20 all 4 cases separate to show the effect of droplet loading on the mean mixture fraction. The increase in mixture fraction of the spray case is due to evaporation of spray droplets. As the droplet loading is increased the mixture fraction also increases.

Radial profiles of the rms fluctuations of mixture fraction, ξ' are shown in Figure 8 for five axial locations in the jets. At the jet exit plane all the profiles show similar trends with peak fluctuations at the edge. A transition can be seen on the jet centre line going from x/D = 0.5 to x/D = 20 where case LA and LL have higher ξ' at lower x/D and case LM and LH has higher ξ' at x/D greater than 10 . At the edge of the jet at x/D = 20, case LM and LH, are showing large fluctuations of mixture fraction when compared with case LA. It is also interesting to note from the profiles shown here that the droplets generate turbulence as evident from the higher peaks obtained in ξ'for the cases with increasing droplet loadings.

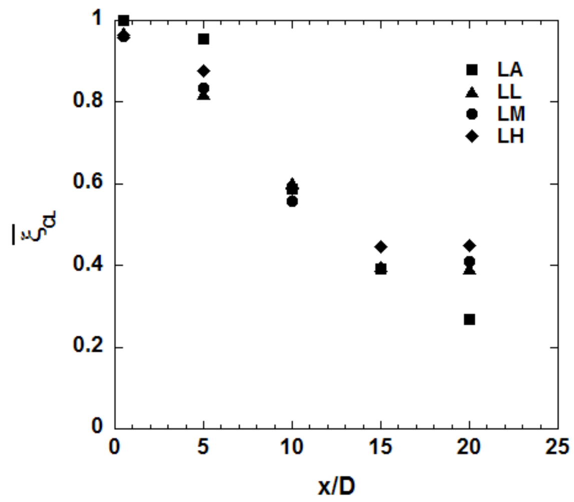

Figure 4. Mean centreline decay of mixture fraction for cases LA LL LM and LH.

Future work on this project aims to study the interactions between the turbulence, droplet and mixture fraction fields. This requires carrying out additional measurements of droplet size distribution and velocity and turbulence field. Using these measurements combined with those presented here for mixture fraction, the evaporation rates may be extracted. Such estimates would be extremely useful for validating the sub-models currently used for the droplet evaporations rates.

Conclusions

This study has shown that the NO LIF technique used in this paper to determine the mixture fraction of the vapour phase in a spray loaded jet is a valid technique. The data presented is a major step forward in creating a database for modellers to model a simple axisymmetric jet loaded with spray droplets.

This study has provided profiles of mean and rms of mixture fraction in spray jets with varying droplet loading. It has been shown that increasing the droplet loading increases the mixture fraction. The increase in mixture fraction in a spray jet is due to evaporation of spray droplets. The turbulent fluctuation also increased as the droplet loading was increased. The evaporation rate could not be determined due to the unavailability of droplet and velocity data.

Acknowledgments

This work is supported by a grant from the Australian Research Council.

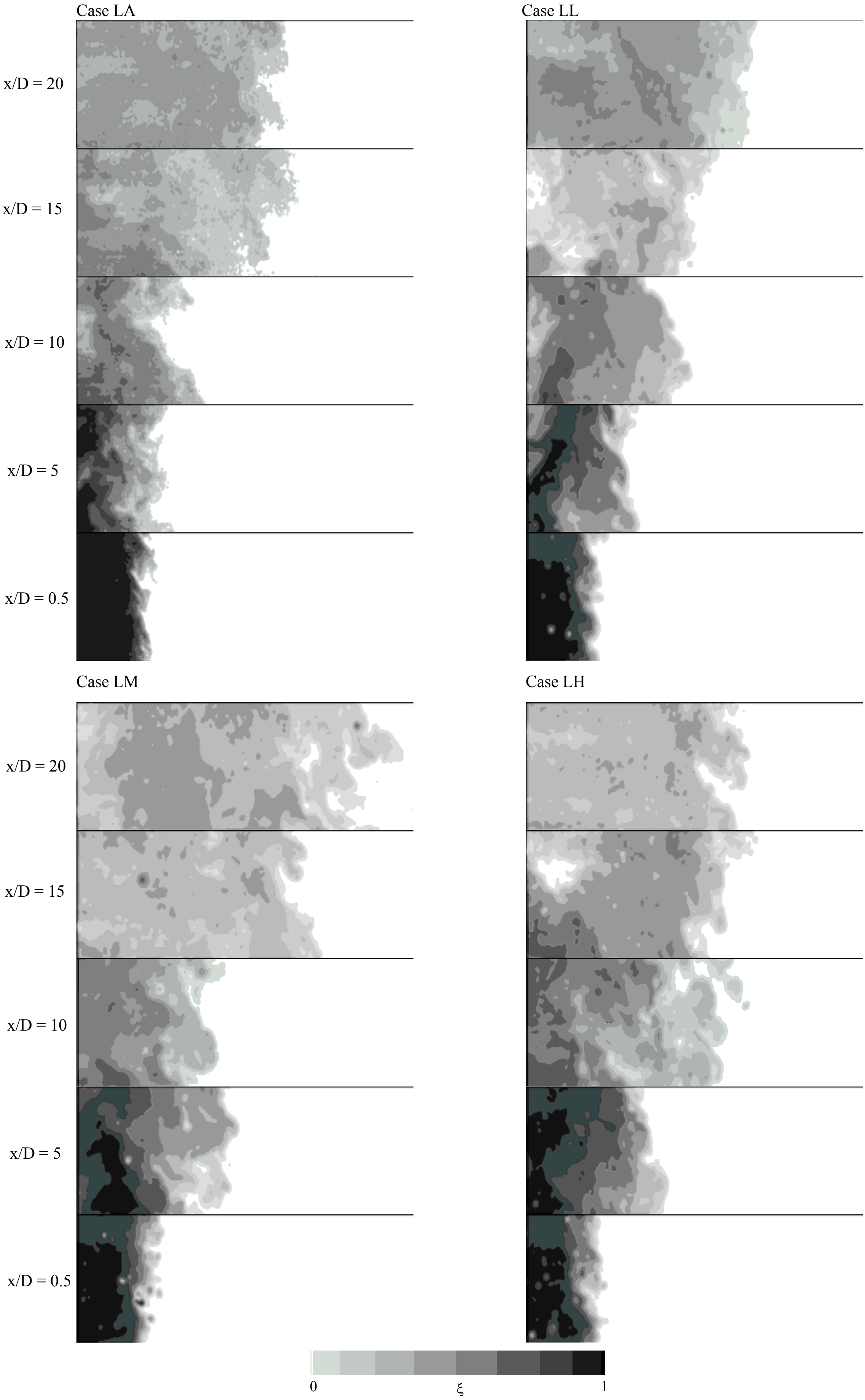

Figure 5. 2D Instantaneous image of mixture fraction for case LA,LL,LM and LH at axial positions of x/D = 0.5, 5, 10, 15 and 20

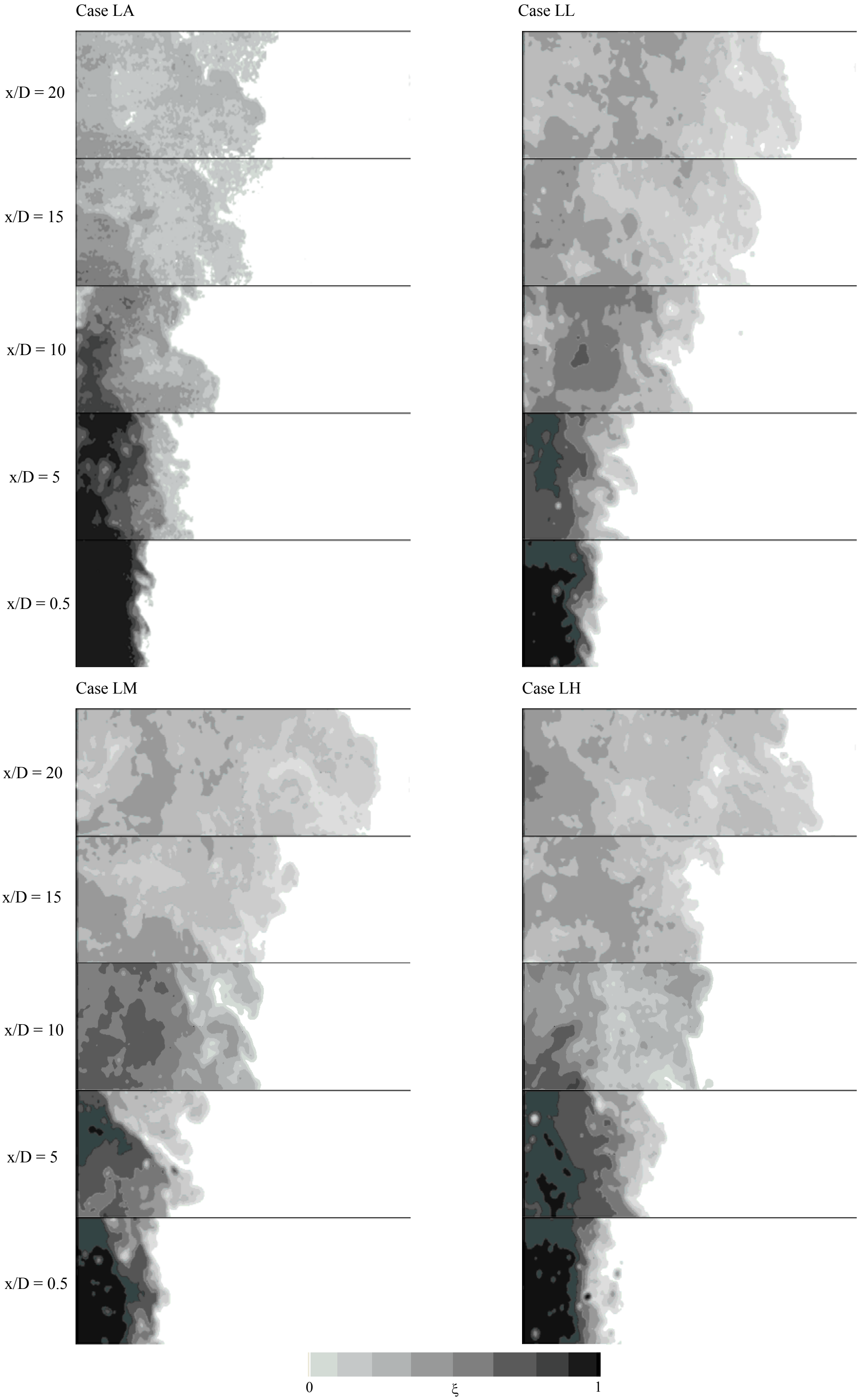

Figure 6. 2D Instantaneous image of mixture fraction for case LA LL LM and LH at axial positions of x/D = 0.5, 5, 10, 15 and 20.

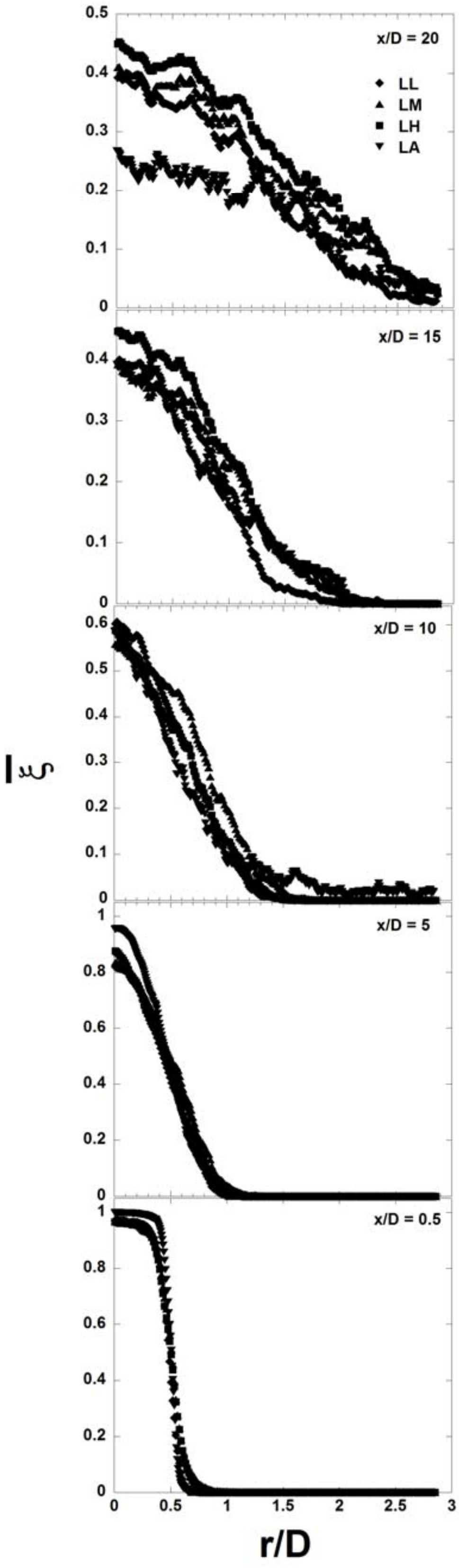

Figure 7. Radial profiles of mean mixture fraction for cases LL, LM, LH, and LA at axial potion of 0.5, 5, 10, 15 and 20.

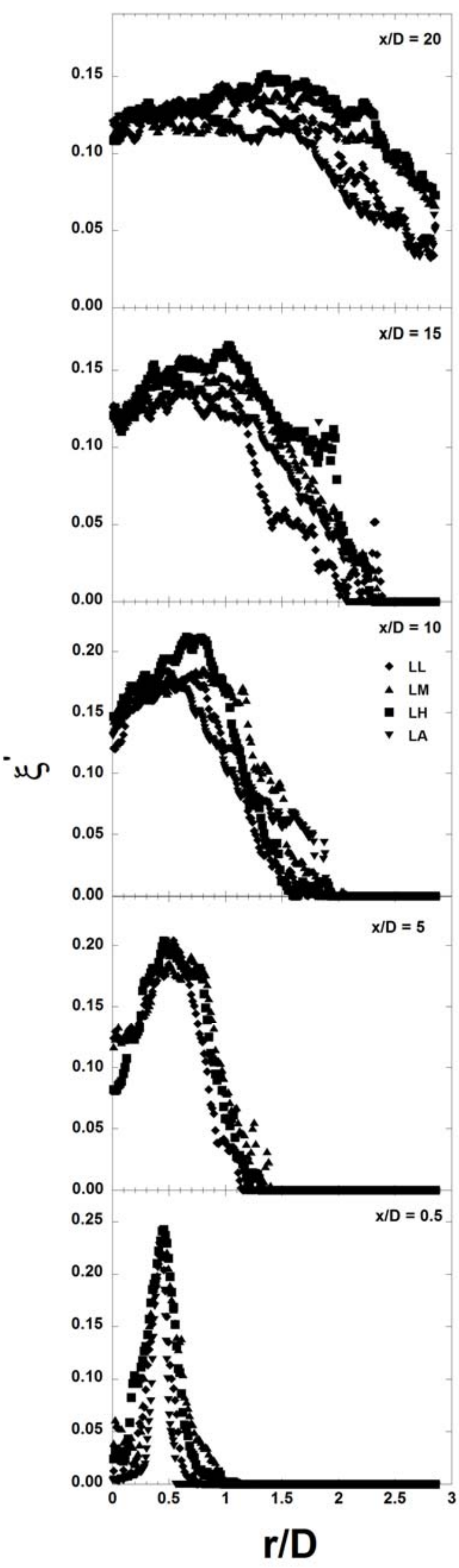

Figure 8. Radial profiles of mixture fraction rms for cases LL, LM, LH, and LA at axial potion of 0.5, 5, 10, 15 and 20.

References

[1] Faeth, G.M., Current Status of Droplet and Liquid Combustion. *Prog. Energy Combust. Sci.*,**3**,1977, 191-224.

[2] Faeth, G.M., Evaporation and Combustion of Sprays. *Prog. Energy Combust. Sci.*, **9**, 1983, 1-76.

[3] Chen Y-C., Starner, S.H. & Masri. A.R., Combined PDA/LIF measurements in Simple, Evaporating Turbulent Spray Jets, in *Proc. 14th Australasian Fluid Mechanics Conference*. 2001, 267-270.

[4] Chen, Y.-C., Starner, S.H. & Masri. A.R., Characteristics of turbulent spray combustion in a piloted jet flame burner. in *Twenty-Ninth International Symposium on Combustion,* **29**, 2002, 625-632.

[5] Starner, S.H., Chen, Y.-C., and & Masri. A.R., Mass Flux Measurements in Simple, Evaporating Turbulent Spray Jets, in *Proc. Third Asia-Pacific Conference on Combustion*. 2001, 331-334.

[6] Starner, S.H. & Masri, A.R., An Experimental Comparison of Evaporating and Non-evaporating Sprays in a Simple Turbulent Jet Flow, in *Proc. 9th International Conference on Liquid Atomization and Spray Systems*. 2003.

[7] Starner, S.H., Gounder, J.D., & Masri, A.R., Effects of turbulence and carrier fluid on simple, turbulent spray jet flames. *Combustion and Flame*, **143**(4), 2005, 420-432.

[8] Gounder, J.D., Masri, A.R, Starner, S.H., & Bilger, R.W., Mixture Fraction Imaging in a Non-Reacting Spray Jet., in *6th Asia-Pacific Conference on Combustion,*. 2007.

[9] Bilger, R.W., Turbulent flows with nonpremixed reactants, in *Turbulent Reacting Flows*. **44**, 1979, 65-113.

[10] Carter, C.D. & Barlow, R.S., Simultaneous Measurements of NO, OH, and the Major Species in Turbulent Flames, in *Optics Letters*, **19,** 1994, 299-301.

[11] Barlow, R.S., Karpetis, A. N., Frank, J. H. & Chen, J. -Y., Scalar profiles and NO formation in laminar opposed-flow partially premixed methane/air flames, *Combustion and Flame*, **127**(3), 2001, 2102-2118.

[12] Naik, S.V., & Laurendeau, N.M., LIF Measurements and Chemical Kinetic Analysis of Nitric Oxide Formation in High-Pressure Counterflow Partially Premixed and Nonpremixed Flames, *Combustion Science and Technology*, **176**(11), 2004, 1809-1853.

[13] Ravikrishna, R.V., & Laurendeau, N.M., Laser-induced fluorescence measurements and modeling of nitric oxide in counterflow partially premixed flame, *Combustion and Flame*, **122**(4), 2000, 474-482.

[14] Ravikrishna, R.V., Sameer, V. N., Cooper, C. S., & Laurendeau, N. M., Quantitative Laser-Induced Fluorescence Measurements and Modelling of Nitric Oxide in High-Pressure Counterflow Diffusion Flames, *Combustion Science and Technology*, **176**(1), 2004, 1-21.

[15] Tamura, M., Luque, J., Harrington, J. E., Berg, P. A., Smith, G. P., Jeffries, J. B., & Crosley, D. R., Laser-induced fluorescence of seeded nitric oxide as a flame thermometer, *Applied Physics B: Lasers and Optics*, **66**(4), 1998, 503-510.

[16] Thomsen, D.D., and Laurendeau, N.M., LIF measurements and modeling of nitric oxide concentration in atmospheric counterflow premixed flames, *Combustion and Flame*, **124**(3), 2001, 350-369.

[17] Kronemayer, H., Bessler, W.G., & Schulz, C., Gas-phase temperature imaging in spray systems using multi-line NO-LIF thermometry, *Applied Physics B: Lasers and Optics*, **81**(8), 2005, 1071-1074.

[18] Antonia, R.A., Browne, L. W. B., Chambers, A. J., & Rajagopalan, S., Budget of the temperature variance in a turbulent plane jet, *International Journal of Heat and Mass Transfer*, **26**(1), 1983, 41-48.

[19] Pitts, W.M., Effects of global density ratio on the centerline mixing behavior of axisymmetric turbulent jets, *Experiments in Fluids*, **11**(2), 1991, 125-134.

[20] Pitts, W.M., Reynolds number effects on the mixing behavior of axisymmetric turbulent jets, *Experiments in Fluids*, **11**(2), 1991, 135-141.

[21] Mi, J., Nathan, G.J., & Nobes, D.S., Mixing Characteristics of Axisymmetic free Jets From a Contoured Nozzle, an Orifice Plate and a Pipe. *Transactions of the ASME*, **123,** 2001, 878-883.

[22] Dally, B.B., Fletcher, D.F., & Masri, A.R., Flow and mixing fields of turbulent bluff-body jets and flames, *Combustion Theory and Modelling*, **2**(2), 1998, 193-219.